J Mol Med (2011) 89:877–889
DOI 10.1007/s00109-011-0774-y

ORIGINAL ARTICLE

Autophagy suppression promotes apoptotic cell death in response to inhibition of the PI3K—mTOR pathway in pancreatic adenocarcinoma

Olga K. Mirzoeva · Byron Hann · Yun K. Hom · Jayanta Debnath · Dana Aftab · Kevan Shokat · W. Michael Korn

Received: 19 January 2011 / Revised: 16 April 2011 / Accepted: 20 April 2011 / Published online: 16 June 2011

Abstract Targeting of pathways downstream of RAS represents a promising therapeutic strategy for pancreatic cancer, the fourth leading cause of cancer-related death in the USA, since activation of the Raf-MEK-ERK and PI3K-AKT pathways is found frequently in this disease and is associated with poor prognosis. Taking advantage of a panel of human PDAC cell lines and specific inhibitors of PI3K and/or mTOR, we systematically address the question whether dual-targeted inhibition of the PI3K and mTOR pathways offers advantages over single-targeted inhibition of PI3K in PDAC. We observe greater overall susceptibility of cell lines to dual inhibition compared to targeting PI3K alone. However, we find that dual inhibition of PI3K and mTOR induces autophagy to a greater extent than inhibition of each target alone. In agreement with this, we show that combined administration of PI3K/mTOR and autophagy inhibitors results in increased anti-tumor activity in vitro and in vivo in models of pancreatic adenocarcinoma. XL765, a PI3K/mTOR inhibitor used in our in vivo studies, is currently undergoing clinical evaluation in a variety of cancer types, while the autophagy inhibitor chloroquine is a widely used anti-malaria compound. Thus, our studies provide rationale for clinical development of combinations of these compounds for the treatment of pancreatic adenocarcinoma.

Keywords PI3K · mTOR · Pancreatic adenocarcinoma · EGFR pathway · Cancer signal transduction · Autophagy · Apoptosis · Chloroquine

Abbreviations

PDAC	Pancreatic ductal adenocarcinoma
PI3K	Phosphoinositide-3 kinase
mTOR	Mammalian target of rapamycin
GI50	Drug concentration inducing 50% growth inhibition
LC50	Drug concentration inducing 50% lethality
AVO	Acidic vesicular organelles
3-MA	3-Methyladenine
CQ	Chloroquine

Electronic supplementary material The online version of this article (doi:10.1007/s00109-011-0774-y) contains supplementary material, which is available to authorized users.

O. K. Mirzoeva · W. M. Korn
Divisions of Gastroenterology and Hematology/Oncology, Department of Medicine, University of California San Francisco, San Francisco, CA, USA

B. Hann · Y. K. Hom · W. M. Korn
Helen Diller Family Comprehensive Cancer Center, University of California San Francisco, San Francisco, CA, USA

J. Debnath
Department of Pathology, University of California San Francisco, San Francisco, CA, USA

D. Aftab
Exelixis, Inc, South San Francisco, CA, USA

K. Shokat
Department of Cellular and Molecular Pharmacology, University of California San Francisco, San Francisco, CA, USA

W. M. Korn (✉)
UCSF Divisions of Gastroenterology and Hematology/Oncology, Department of Medicine, Helen Diller Family Comprehensive Cancer Center, 2340 Sutter St., Box 1387, San Francisco, CA 94115, USA
e-mail: Michael.Korn@ucsf.edu

Introduction

The hallmark molecular alterations in pancreatic ductal adenocarcinoma (PDAC) are activating mutations of the KRAS oncogene, resulting in constitutive activation of effector pathways [1, 2]. The KRAS protein is widely considered to be "undruggable" [3]. Therefore, RAS-effector pathways, the RAF-MEK-ERK and PI3K pathways, in particular, have emerged as high-priority therapeutic targets. Both pathways represent promising therapeutic targets in pancreatic cancer, since presence of phosphorylated ERK and AKT is found frequently [4, 5] and is associated with poor prognosis [6]. Initial clinical observations with selective inhibitors of MEK and PI3 kinase (PI3K) have demonstrated limited tumor activity [7, 8], a possible consequence of insufficient patient selection strategies and incomplete information about the complexity of the targeted molecular networks.

The type-I PI3-Ks (p110α, p110β, p110γ, and p110δ) transmit signals through synthesis of phosphatidylinositol-3,4,5-triphosphate (PIP3), which mediates activation of downstream targets, including AKT. The importance of PI3K for tumor development and progression has led to the generation of an increasing number of specific PI3K inhibitors. While some of these agents target PI3K selectively, a number of compounds exhibit dual activity against PI3Ks and the PIKK mTOR, which controls cell growth [9–11]. Despite the well-documented role of PI3K in suppressing apoptosis in cancer cells, initial experience with dual-targeted PI3K/mTOR inhibitors in preclinical models of glioblastoma demonstrated predominantly anti-proliferative effects [12]. In breast cancer, apoptosis occurred only in cells harboring HER2 amplification or PIK3CA mutations [13]. In primary xenograft tumors derived from human PDAC, significant inhibition of tumor growth with only minimal induction of apoptosis by the pan-PI3K/mTOR inhibitor NVP-BEZ325 was observed [14].

With the work presented here, we explore whether dual-targeted inhibition of the PI3K and mTOR pathways offers advantages over single-targeted inhibition of PI3K in PDAC and investigate the consequences of cooperative effects of PI3K and mTOR on autophagy. We show that combined administration of PI3K/mTOR and autophagy inhibitors enhances anti-tumor activity in vitro and in vivo in models of pancreatic adenocarcinoma, thus providing a basis for rational combination of these compounds for the treatment of pancreatic adenocarcinoma.

Materials and methods

Reagents Chemical synthesis and characterization of PI3K inhibitors PI-103 and PIK90 are described by Knight and colleagues [15]. The following reagents were used: Rapamycin (Calbiochem), EGF (Millipore). CI1040 (PD184352) was provided by Dr Bain (University of Dundee, UK), XL765 and XL147 were provided by Exelixis, Inc. All drugs were diluted in DMSO except for PIK90 which was diluted in DMSO/H2O 1:1 (*v*/*v*). The following antibodies were used: pS6 (S240/244), p4EBP1 (Thr37/46), pS6K (Thr389), pAkt (S473), total Akt, beta-actin (Sigma), LC3 (Abcam ab51520). *N*-benzyloxy-carbonyl-Val-Ala-Asp-fluoromethylketone (z-VAD-fmk; R&D Systems), 3-MA, acridine orange; chloroquine diphosphate was from MP Biomedicals, protease inhibitors cocktail set III; E-64d, pepstatin A were from Calbiochem.

Cell culture Pancreatic cancer cell lines were kindly provided by S. Gysin, M. McMahon, and E. Collisson (UCSF, San Francisco, CA, USA). The cells were described previously [16]. All cells were cultured in high-glucose DMEM supplemented with 10% FBS (US origin, Valley Biomedical).

Cell growth inhibition assays Cells were plated in 96-well plates (density from 2,000 to 6,000 cells per well). Cells were allowed to attach overnight before drug treatment for 72 h. Increasing doses of each drug in 1:2 serial dilutions were added in triplicate wells. Each inhibitor was initially screened at large dose ranges, up to maximal concentration achievable under tissue culture conditions. The drugs had different solubility in tissue culture medium, and therefore, the maximal dose for PI103 was 5 μM, whereas other drugs were screened up to 20 μM. The final DMSO concentration was 0.2% or less. Cell viability was determined using the CellTiter-Glo (CTG) assay (Promega, Madison, WI, USA) at day 0 (before the drug treatment) and at day 3 post-drug exposure. Growth inhibition parameters (GI50, LC50) were calculated as described before [17].

Apoptosis and autophagy analyses Cells were treated with drugs 24 h after plating and harvested for apoptosis or autophagy assays at 1, 2, or 3 days after drug treatment. Apoptosis was measured using the Apoptosis Detection Kit I (BD Pharmingen) and quantified by Flow Cytometry (FACS Calibur, BD) using the CellQuest software. All treatments were done in triplicates and at least 20,000 cells were acquired from every sample.

Analysis of punctate GFP-LC3 was done in MIAPaCa-2 and Panc10.05 cells stably expressing a GFP-LC3 fusion construct [18]. Briefly, the cells were plated on glass coverslips; 24 h later, they were treated with drugs and fixed with 2% paraformaldehyde at 48 and 72 h after drug exposure.

Cells were viewed in Vectashield mount medium (Vector Lab, Inc.) under a Zeiss Axioplan 2 fluorescent microscope

using 100× 1.3 NA objective and photographed by Zeiss AxioCam HR camera using Axiovision 4.7 Software.

Acidic vesicular organelles (AVOs) were detected in drug-treated cells by vital staining with acridine orange. Acridine orange was added to the cells (1 μg/mL) for 15 min, then washed off with PBS and phenol red-free growth medium was added. The cells were examined and photographed using an inverted fluorescent microscope Zeiss Axiovert S100TV at 40×/0.6 NA using DCM 200 digital camera and ImageJ software. To quantify the development of AVOs, the acridine orange-stained cells were trypsinized, washed, resuspended in phenol red-free growth medium and analyzed at the FACSCalibur. The degree of AVO formation was expressed as fold increase of acridine orange fluorescence intensity (FL3) in drug-treated cells versus control cells.

Preparation of protein lysates and Western blot analysis The cells were treated with drugs 48 h after plating and harvested at 4 h post-drug exposure. Protein lysates were prepared from cells at 70–90% confluency. For detection of autophagy by LC3-II expression, the lysates were prepared 48 h post-drug treatment. To further assess autophagic flux, we detected LC3-II levels in both control and drug-exposed cells treated with lysosomal cathepsin inhibitors E64d (5 μg/ml) and pepstatin A (10 μg/ml) which were added to the culture medium 2 h before lysis. Autophagy inhibitor 3-MA was added at 3.5 mM 1 h before the drugs. Western blot analysis was performed as described previously [17].

In vivo xenograft tumor studies Female 7 to 9-week-old Nu/Nu mice (Harlan, FoxN1/nude) were inoculated s.c. with 10^7 BxPC-3 cells. Mice were monitored according to the protocol approved by the University of California, San Francisco Institutional Animal Care and Use Committee. When tumors reached about 100 mm^3, mice were randomly assigned to one of six treatment groups: vehicle control, XL765 30 mg/kg, XL147 100 mg/kg, Chloroquine (CQ) 50 mg/kg, XL765+CQ, and XL147+CQ. XL765 was solubilized in water/10 mM HCl, XL147 was dissolved in water, both drugs were administered by oral gavage once a day, five times a week. CQ was dissolved in saline and injected i.p. daily, five times a week. Each treatment regimen was tested in cohorts of eight mice, and the dosing was continued for 28 days. Tumor sizes were measured twice weekly in two dimensions using a caliper, tumor size (cubic millimeter) was calculated as (length × $width^2$)/2. The doses for drug treatments were chosen as MTD according to a preceding toxicity study in mice bearing BxPC-3 xenografts. Animals were monitored for the absence of drug toxicity by monitoring body weight and overall activity.

Statistical analysis Data are expressed as mean±standard deviation. Statistical analysis was performed by using Student's t test (two-tailed). P values of <0.05 were considered significant.

Results

Greater inhibition of cell growth by dual PI3K/mTOR inhibitors compared to PI3K-selective inhibitors in a panel of PDAC cell lines The effect of two PI3K-selective inhibitors (XL147, PIK90) and the two dual-targeted PI3K/mTOR inhibitors (XL765 and PI-103) on cell viability was tested in 13 PDA cell lines by treating cells at increasing drug doses. As shown in Fig. 1a, a broad spectrum of sensitivities was observed. Interestingly, the dual-targeted PI3K/mTOR inhibitor XL765 induced cell killing in many more cell lines (as indicated by negative survival rate) and at lower concentrations as compared to the single-targeted inhibitors XL147 and PIK90. Supplementary Table 1 summarizes GI50 and LC50 (drug concentrations inducing 50% growth inhibition and 50% lethality, respectively) for four drugs. In more cell lines (6 out of 13), the LC50 was reached after treatment with XL765, as compared to the other drugs. A comparative analysis of relative sensitivity to the four inhibitors between all the cell lines revealed that individual cell lines tended to demonstrate similar relative sensitivity to all inhibitors. In agreement with this, sensitivities for XL147, XL765, and PIK90 were strongly correlated, while the correlation with sensitivity to PI103 was weak. For PI103, a subset of pancreatic cancer cell lines (e.g., BxPC-3, HuP-T3, HPAF-II) displayed weak or no growth inhibition, and we were not able to determine the GI50 for them. Assessment of pAKT levels in PI103-resistant cell lines by Western blot analysis demonstrated no inhibition of PI3K signaling after PI103 treatment, while other PI3K inhibitors clearly inhibited phosphorylation of AKT in these cells (Supplementary Fig. 1 and data not shown). In addition, PI103-resistant cell lines demonstrated suppression of pAkt and cell growth inhibition when dual PI3K/mTOR inhibition was achieved by combining PIK90 and rapamycin. It is conceivable that PI103 becomes rapidly inactivated in these cells, e.g., through active elimination of the drug. This possibility is currently under investigation in our laboratory. In summary, these data demonstrate a drug-class effect on cell viability that is independent of the activity of individual compounds.

Synergistic induction of apoptotic cell death through inhibition of PI3K and mTOR To determine whether the effect of inhibitors on PDAC cell viability was due to cell killing, we measured apoptosis induction by Annexin V/PI

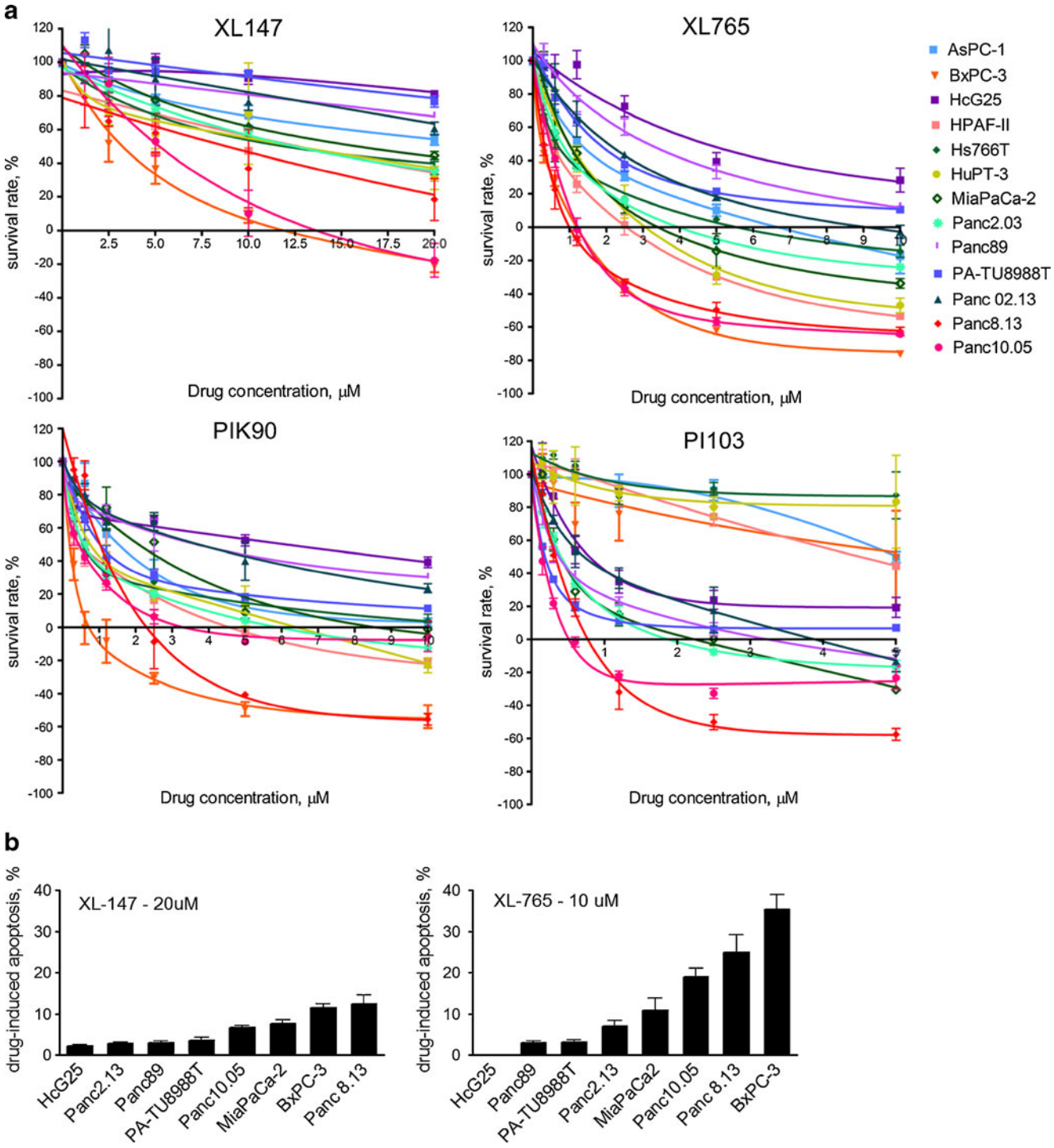

Fig. 1 Comparison of sensitivity of pancreatic cancer cell lines to single PI3K and dual PI3K/mTOR inhibitors. **a** Drug dose-response of cell growth inhibition. Thirteen pancreatic cancer cell lines were treated with increasing doses of the indicated inhibitors and the cell viability was assessed at day 0 (time of drug addition) and at day 3 after treatment using ATP-based cell viability assay (Promega). Percentage of growth inhibition at each drug dose was calculated as described in Materials and methods. **b** Apoptosis response induced by single PI3K inhibitor XL147 and dual PI3K/mTOR inhibitor XL765 in pancreatic cancer cells. Apoptosis was determined by total percentage of annexin V-positive cells by fluorescence-activated cell sorting (FACS). The apoptosis rate of the untreated control cell population was subtracted from the drug-treated population to determine the drug-induced apoptotic cell fraction. *Columns*, mean of duplicates; *bars*, SD. For each duplicate, 40,000 cells were acquired

staining. As shown in Fig. 1b, treatment with XL147 and XL765 resulted in different degree of apoptosis induction in pancreatic cancer cell lines. Similar data were obtained with PIK90 and PI103 (data not shown). The highest degree of apoptosis was achieved by treatment with the dual PI3K/mTOR inhibitor XL765 and the apoptotic response was inversely correlated with GI50 (Supplementary Fig. 2), suggesting apoptosis as a likely mechanism underlying cell death observed in the cell viability assay. To test whether simultaneous inhibition of PI3K and mTOR with individual compounds led to enhanced cell killing compared to inhibition of each target alone, cells were treated with combinations of the PI3K inhibitors PIK90 or XL147 with the mTORC1 inhibitor rapamycin and the mTOR kinase inhibitor PP242 (inhibiting mTORC1 and mTORC2) [9]. As demonstrated in Fig. 2a, treatment with the drug combinations

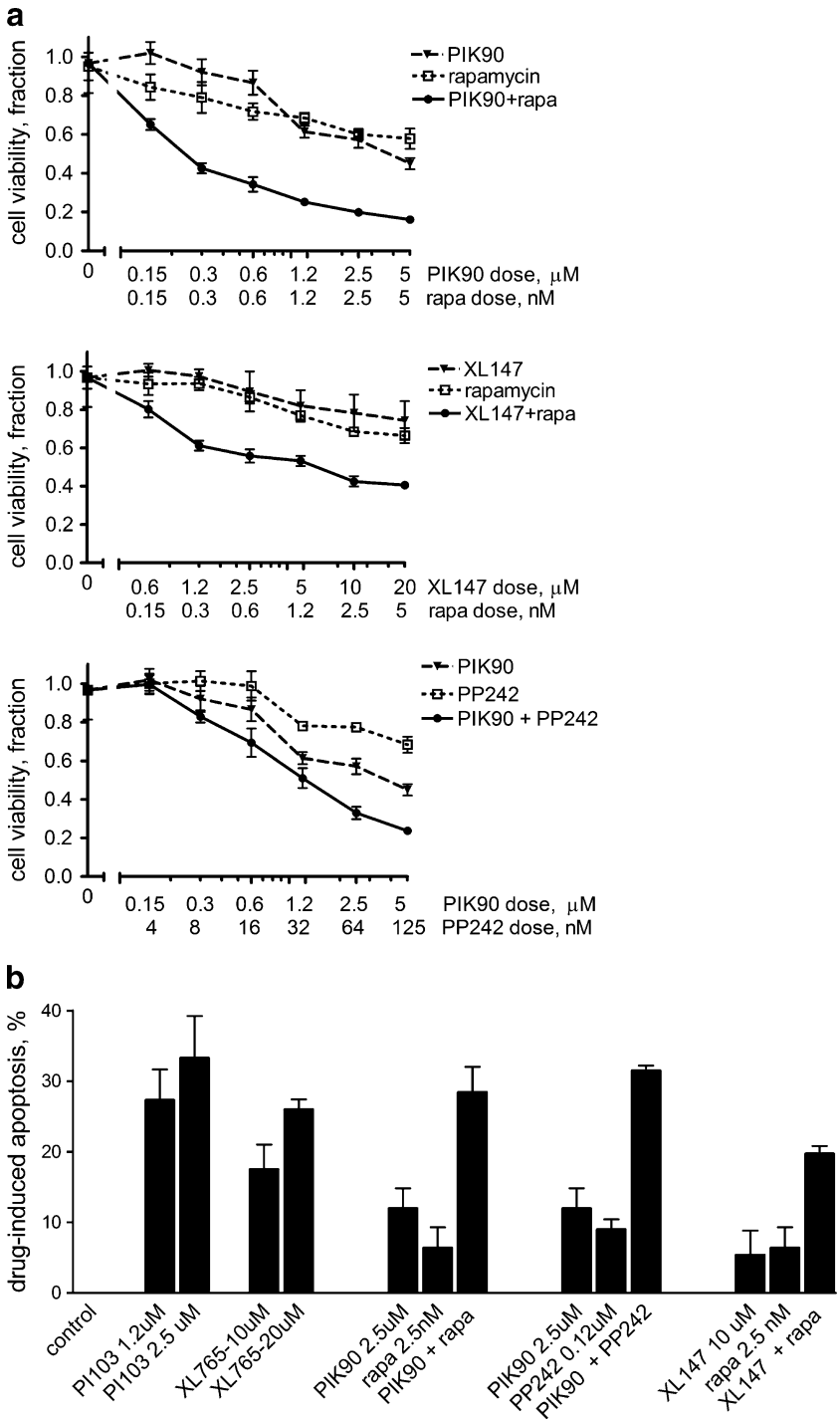

Fig. 2 Synergistic effect of combinations of PI3K and mTOR inhibitors on cell viability (**a**) and apoptosis (**b**) of pancreatic cancer cell line MiaPaCa-2. **a** Dose/effect curves for each inhibitor and their combinations at fixed molar ratio are presented. Cell viability was measured at 72 h after treatment with the drugs. Relative cell viability of drug-treated cells was calculated as a fraction of vehicle-treated control. *Points*, mean of triplicates; *bars*, SD. **b** Combinations of different PI3K/mTOR inhibitors result in synergistic induction of apoptosis reaching the same rate as induced by dual PI3K/mTOR inhibitors PI-103 and XL765. Apoptosis was determined by FACS analysis as a total number of annexin V-positive cells. Drug-induced apoptosis was calculated by subtraction of apoptosis of control cells from that of drug-treated cells. *Columns*, mean of duplicates; *bars*, SD. For each duplicate, 40,000 cells were acquired. The results were confirmed in at least two independent experiments

resulted in potentiation of cell growth inhibition. In agreement with these findings, combined PI3K/mTOR inhibition also markedly increased the levels of apoptosis (Fig. 2b). These data clearly demonstrate that dual inhibition of both, PI3K and mTOR, results in enhanced cell growth inhibition and apoptotic cell death compared to inhibition with single-targeted agents. Additionally, this effect can be recapitulated by using combinations of single-targeted compounds. It is also important to note that the mTORC1/mTORC2 inhibitor PP242, which also inhibits AKT phosphorylation at Ser-473 through its effect on the mTORC2 complex, is not sufficient for generating the same extent of apoptosis as can be achieved by inhibition of PI3K/mTOR.

Induction of apoptosis depends on pathway inhibition following PI3K inhibition We reasoned that the marked differences between PI3K-selective and dual PI3K/mTOR inhibitors could be explained by differences in inhibition of signaling through the target pathways. Four cell lines with different levels of sensitivity to XL147 and XL765 (based on GI50) were selected, and cells were treated with increasing drug doses for 4 h. Western blot analyses for key proteins involved in PI3K, MEK, and mTOR signaling were performed. The relatively sensitive cell lines BxPC-3 and Panc8.13 demonstrated inhibition of PI3K as determined by reduced levels of pAKT (Ser-473) at low concentrations of the inhibitors (Fig. 3a). In addition, treatment with XL765 reduced phosphorylation of the mTOR targets S6, S6K, and 4EBP1 significantly. This additional inhibition of mTOR activity was associated with greater apoptosis induction compared to PI3K inhibition alone (Fig. 3b). In contrast, PI3K activity was only slightly inhibited in the relatively resistant Panc2.13 cell line with both inhibitors and in PA-TU8988T following treatment with XL765. This finding provokes the question whether inhibition of both pathways is required for induction of apoptosis in pancreatic cancer cells. Indeed, treatment of PA-TU8988T cells with XL147 and rapamycin abolished phosphorylation of AKT, S6, S6K and significantly reduced p4EBP1, which was associated with a significant increase in apoptosis rate (Fig. 3d, e). None of the compounds tested prevented phosphorylation of AKT in Panc2.13 cells. This was also true for TGX115, a preferential inhibitor of p110β [15]. The mechanism underlying resistance to PI3K inhibition in this cell line is currently under investigation.

Autophagy induction as a mediator of sensitivity to PI3K inhibitors in PDA cell lines Since mTOR is a strong suppressor of autophagy [19, 20], we reasoned that treating pancreatic cancer cells with PI3K/mTOR inhibitors could result in autophagy. To detect the development of AVOs, MIAPaCa-2 cells were treated with inhibitors for 1–3 days and then stained with acridine orange. Drug-treated cells showed abundant lysosomal acidity which was reflected by bright red fluorescence emitted by acridine orange (Fig. 4a). In addition, monodansylcadaverine staining demonstrated accumulation of autophagosomes in MIAPaCa-2 cells after treatment with PI103 and XL765 (data not shown). We also evaluated changes in cellular distribution of the autophagy marker LC3. Two pancreatic cancer cell lines: MIAPaCa-2 and Panc10.05 stably expressing a LC3-GFP construct were generated. As illustrated in Fig. 4b, PI103 caused an accumulation of LC3 in a punctate fluorescent pattern, indicating the redistribution of LC3 to autophagic vacuoles, whereas most of the untreated cells manifested a diffuse staining. Furthermore, we examined the PE-lipid conjugation of endogenous LC3 in cell lysates from drug-treated cells; the PE-modification of LC3 results in a faster migrating isoform LC3-II that can be detected by immunoblotting [21]. An increased level of LC3-II was observed in MIAPaCa-2 cells at 72 h post-treatment with PI103 (Fig. 4c), XL765 or XL147 (Fig. 4f). 3-Methyladenine (3.5 mmol/L), which inhibits autophagosome sequestration [22, 23] suppressed levels of the LC3-II form (Fig. 4c). Since LC3-II is subject to lysosomal degradation during autophagy, we assessed LC3-II levels in cells treated with lysosomal cathepsin inhibitors E64d and pepstatin A (lanes labeled E/P). These experiments confirmed increased LC3-II turnover resulting from cell exposure to dual PI3K/mTOR inhibition.

To further understand whether efficient induction of autophagy depends on inhibition of both, PI3K and mTOR, we treated a panel of pancreatic cancer cells with the dual-targeted inhibitor XL765, selective PI3K inhibitor XL147, or a combination of XL147 and rapamycin. We quantified lysosomal acidity as a surrogate for the induction of autophagy by analyzing cells stained with acridine orange by flow cytometry. We compared fluorescence intensity of acridine orange in drug treated versus control cells. As demonstrated in Fig. 4d–f, treatment with the dual inhibitors XL765 and PI103 resulted in significant dose-dependent AVO induction and LC3-II stimulation. The selective PI3K inhibitor XL147 also induced AVOs, although to a lesser extent than XL765. Treatment with the mTOR inhibitor rapamycin at doses lower than 5 nM resulted in only minimal autophagy. Markedly higher levels of autophagy were observed when PI3K and mTOR inhibitors were combined. In contrast, addition of rapamycin to XL765 did not significantly enhance autophagy (Fig. 4e), in agreement with the fact that the dual inhibitor efficiently inhibits mTOR on its own. Thus, dual inhibition of PI3K/mTOR results in greater autophagy induction than does inhibition of each pathway component alone.

We next assessed the relationship of autophagy and apoptosis in response to the drugs. We measured autophagy by acridine orange staining in a subset of cell lines with

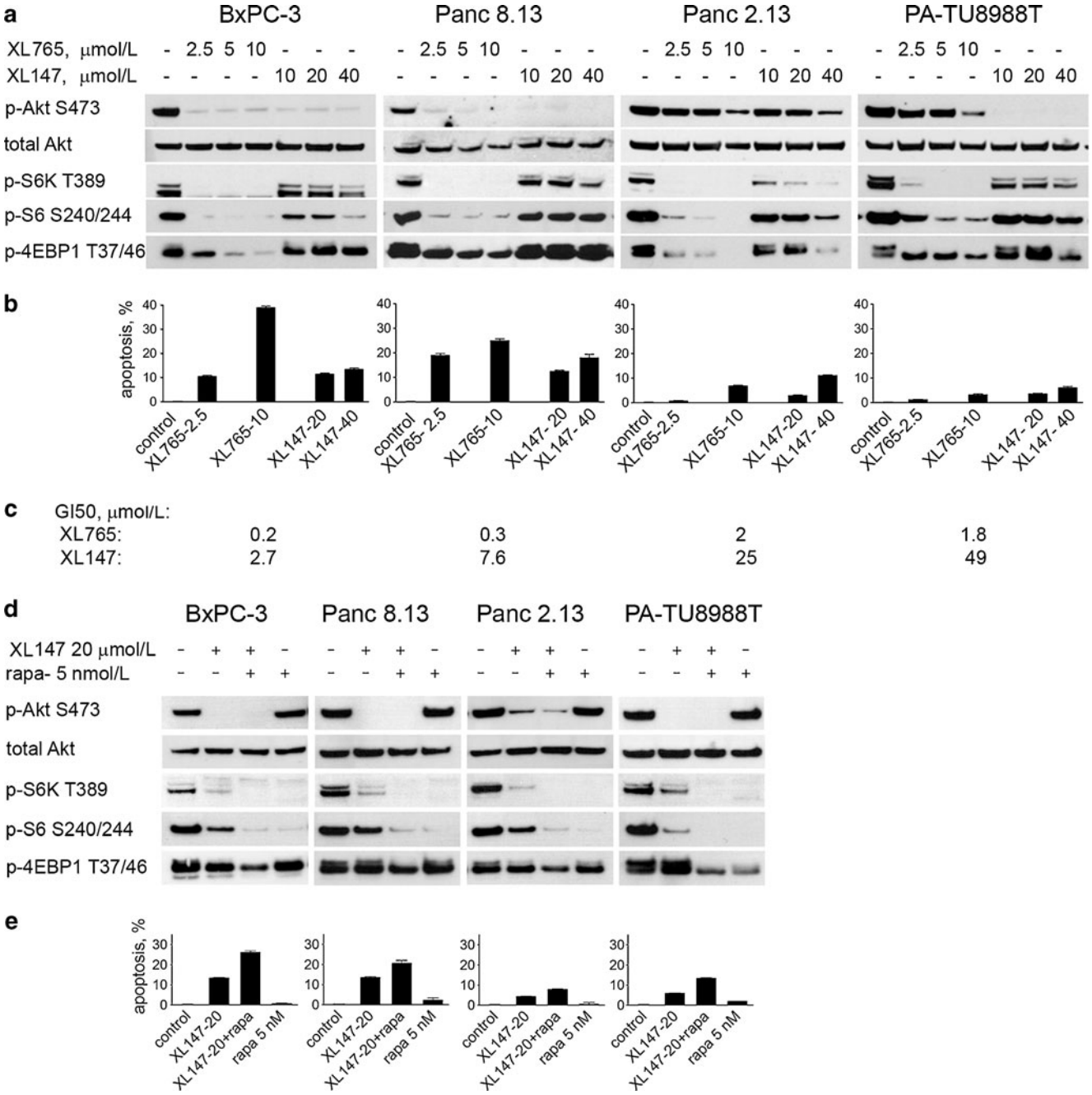

Fig. 3 Differential biochemical and cellular effects of different doses of XL765 and XL147 inhibitors on two sensitive (BxPC-3 and Panc 8.13) and two resistant (Panc 2.13 and PA-TU8988T) cell lines. **a** Representative Western blot analysis of PI3K and mTOR target inhibition at 4 h post-treatment with the indicated doses of drugs. **b** FACS-based analysis was used to determine percentage of apoptotic cells at 72 h after treatment with the indicated doses of drugs. *Columns*, mean of duplicates; *bars*, SD. For each duplicate, 40,000 cells were acquired. **c** GI50 concentrations of XL765 and XL147 for each cell line were determined by cell viability assay at 72 h post-treatment as described in Materials and methods. GI50s are much lower for BxPC-3 and Panc 8.13 (sensitive cells) than for Panc 2.13 and PA-TU8988T (resistant cells). **d** Representative Western blot analysis of PI3K and mTOR target inhibition at 4 h post-treatment with XL147, rapamycin and their combination. **e** Percentage of apoptotic cells at 72 h after treatment with drugs, as determined by FACS analysis. *Columns*, mean of duplicates; *bars*, SD. For each duplicate, 40,000 cells were acquired

different sensitivity to all four inhibitors. Cell lines displaying induction of apoptosis following drug treatment were considered "sensitive", while cell lines without evidence for apoptosis induction were considered "resistant". The resistant cell lines displayed the least degree of autophagy activation as compared to sensitive cell lines

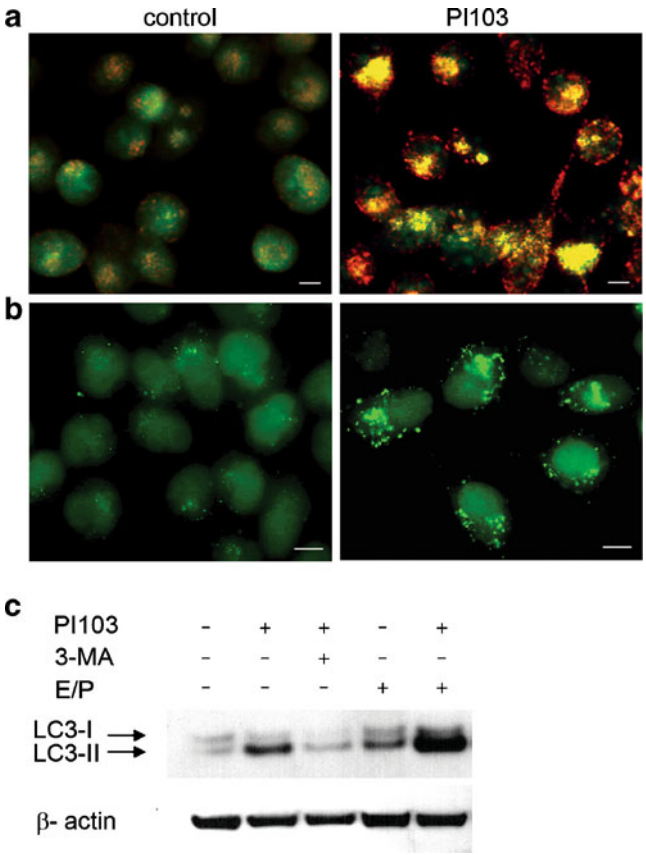

Fig. 4 Dual PI3K/mTOR inhibition induces autophagy in pancreatic cancer cells. **a** Development of acidic vesicular organelles (AVO) in cells after treatment with dual PI3K/mTOR inhibitor. MIAPaCa-2 cells were treated with 1.2 μM of PI103 for 48 h, incubated with acridine orange, washed, and visualized under inverted fluorescent microscope. Red fluorescent granules indicate formation of AVO as described in Materials and methods. **b** Autophagosome formation is induced by dual PI3K/mTOR inhibitor as indicated by LC3-GFP punctated localization. MIAPaCa-2 cells stably expressing LC3-GFP were grown on glass coverslips, treated with 1.2 μM of PI103 for 48 h, fixed and subjected to fluorescent microscopy. Bar, 10 μm. **c** Representative Western blot analysis of LC3-I and LC3-II expression. Cells were pre-treated with autophagy inhibitor 3-MA for 1 h, then PI-103 was added. Cells were lysed at 48 h post-drug treatment for protein extraction. The *E/P lanes* indicate E64d and pepstatin A added directly to the culture 3 h before lysis at 10 μg/ml each. Protein lysates were subjected to immunoblotting with anti-LC3 and anti-β-actin antibodies. **d** Dual PI3K/mTOR inhibitors XL765 and PI103 induce dose-dependent autophagy. Selective PI3K inhibitor XL147 also induces autophagy which is further enhanced by addition of rapamycin. BxPC-3 and Panc10.05 or MIAPaCa-2 **e** cells were treated with indicated drugs for 48 h, then stained with acridine orange and analyzed by FACS. The degree of autophagy was determined as fold change in acridine orange fluorescence intensity (FL3) in drug-treated cells versus the control cells. *Columns*, mean of duplicates; *bars*, SD. For each duplicate, 40,000 cells were acquired. The results were confirmed in at least two independent experiments. **f** LC3-I and LC3-II expression in BxPC-3 cells which were treated with indicated inhibitors for 48 h. The *E/P lanes* indicate E64d and pepstatin A added directly to the culture 3 h before lysis at 10 μg/ml each. The increase in LC3-II expression well correlated with FACS analysis showing autophagy increase in response to PI3K and combined PI3K/mTOR inhibition (especially in the presence of lysosome inhibitors). **g** Autophagy response is higher in drug-sensitive than in resistant cell lines. Three to four sensitive and resistant cell lines were selected for each of the indicated inhibitor on the basis of the degree of their apoptosis response to the inhibitor. The autophagic response of cell lines was compared by FACS analysis of acridine orange staining as described above. Cell lines are distributed as groups of sensitive (*sens*) and resistant (*resist*)

(Fig. 4g). This suggests that in sensitive cell lines, both responses are coactivated as has been described in other systems [24].

Analysis of the temporal relationship between autophagy and apoptosis in time-course experiments demonstrated that induction of autophagy preceded the earliest detectable signs of apoptosis (Fig. 5a). This raised the possibility that autophagy protected cells from cell death by apoptosis. We therefore tested whether inhibitors of autophagy or apoptosis could shift the cellular response from autophagy to apoptosis or vice versa. Inhibition of early stages of autophagy with 3-MA inhibited autophagy but significantly increased the percentage of apoptotic cells (Fig. 5b–d). In contrast, pretreatment of cells with the apoptosis inhibitor z-VAD-*fmk* abolished apoptosis while it further enhanced autophagy induced by the dual-targeted agent PI103. Similar results were obtained with chloroquine, known to inhibit autophagy at late stages (Fig. 6a). When chloroquine

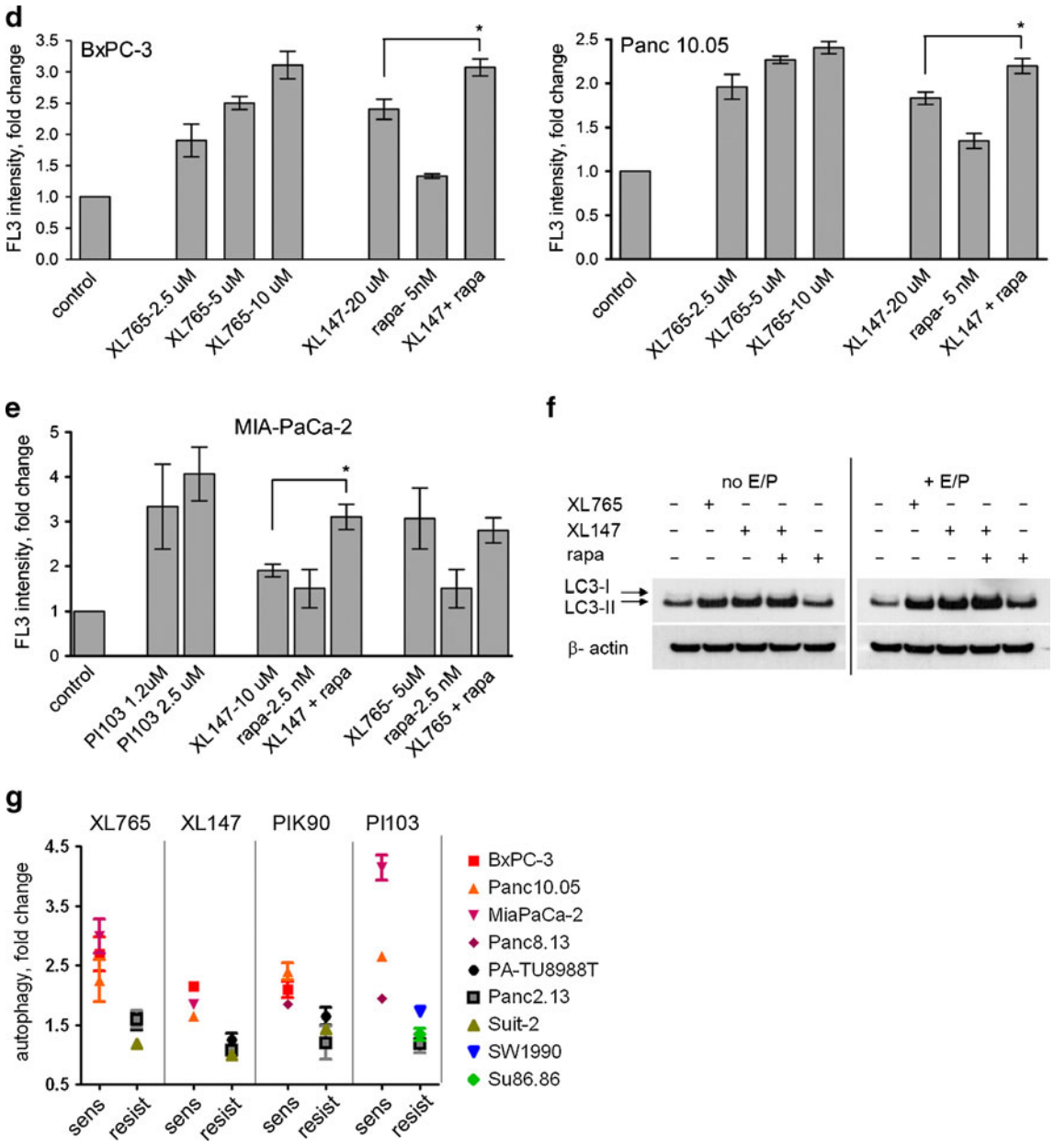

Fig. 4 (continued)

was added to XL765 or to a combination of XL147 and rapamycin, apoptotic cell death was significantly enhanced in a number of cell lines.

Inhibition of autophagy enhances tumor growth inhibition in vivo We next explored whether autophagy inhibition increased the activity of PI3K inhibitors in vivo. Xenograft tumors derived from BxPC-3 cells were grown in the hind flanks of nude mice. Treatment with XL147 and XL765, each alone or in combination with chloroquine, was administered for 28 days. As shown in Fig. 6b, treatment with XL147 resulted in some inhibition of tumor growth that was not enhanced by addition of chloroquine. In contrast, the combination of XL765 with chloroquine resulted in significant inhibition of tumor growth, while XL765 alone at the same dose had no growth inhibitory effect.

Discussion

The present study highlights the PI3K pathway as a valid therapeutic target in pancreatic adenocarcinoma. This is in agreement with the consistent occurrence of *KRAS* muta-

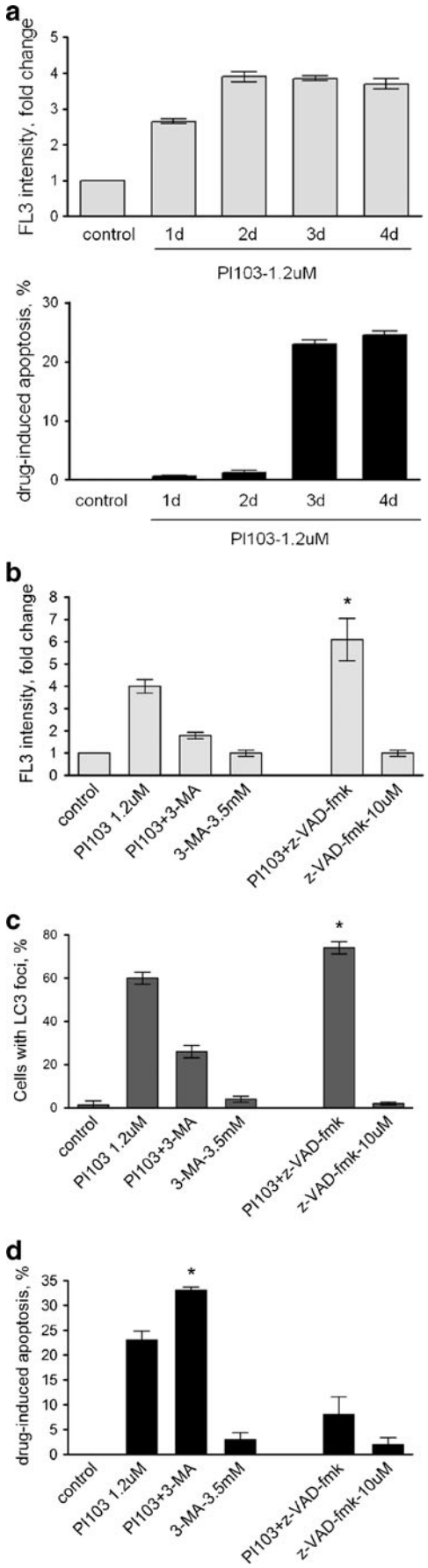

◀ **Fig. 5** **a** Time course analysis of autophagy and apoptosis responses reveals that autophagy precedes apoptosis. MIAPaCa-2 cells were treated with of PI103 (1.2 μM) for 1–4 days and then stained either with acridine orange for detection of autophagy or with annexin V and PI for detection of apoptosis. The degree of autophagy was determined as fold change in acridine orange (FL3) fluorescence intensity of drug-treated cells versus the control cells. Drug-induced apoptosis was determined by subtraction of apoptosis of control cells from that of drug-treated cells. *Columns*, mean of duplicates; *bars*, SD. For each duplicate, 40,000 cells were acquired. **b, c, d** Autophagy/apoptosis interplay: apoptosis is enhanced by autophagy inhibition and autophagy is enhanced by apoptosis inhibition. MIAPaCa-2 or MIAPaCa-2 cells stably expressing LC3-GFP were pretreated with autophagy inhibitor 3-MA or caspase inhibitor z-VAD-fmk for 1 h, then treated with PI103 for 72 h and then subjected to autophagy and apoptosis assays. **b** Supravital staining with acridine orange was performed and cells were analyzed by FACS to determine the fold change in AVO increase. **c** Cells expressing LC3-GFP were fixed and visualized by fluorescent microscopy. At least 200 cells were scored for each treatment to calculate the percentage of cells displaying punctated GFP-LC3 localization pattern such as in Fig. 4b. The percentage of cells displaying LC3-GFP autophagosomes well correlated with autophagy response detected by acridine orange. *Columns*, mean of duplicates; *bars*, SD. The results were obtained in at least three independent experiments. **d** Drug-induced apoptosis as determined by total number of annexin V-positive cells in drug-treated population compared to control population

tions and over-expression of EGFR in this disease, resulting in activation of downstream pathways, including the PI3K and Raf-MEK-ERK pathways. Both pathways intersect at the level of mTOR since AKT and ERK have been demonstrated to phosphorylate TSC2, resulting in derepression of mTOR [25]. Furthermore, MAPK signaling can stimulate mTORC1 activity through p90 ribosomal S6 kinases [26]. Thus, we hypothesized that combined inhibition of PI3K and mTOR might produce superior cell killing in pancreatic cancer compared to inhibition of either target alone through abolishing PI3K and ERK-dependent cell survival signals.

To test this hypothesis, we utilized selective inhibitors of PI3K (XL147 and PIK90) and dual-targeted PI3K/mTOR inhibitors (XL765 and PI103) [15, 27]. We observed that dual inhibition of PI3K and mTOR by XL765 or PI103 resulted in increased apoptosis induction compared to inhibition of each target alone. Furthermore, combinations of selective inhibitors of PI3K with mTOR inhibitors resulted in additive or synergistic increases in apoptosis. These findings are contrasting observations reported for non-small cell lung cancer and glioblastoma where dual inhibition of PI3K and mTOR resulted in growth inhibition but not apoptosis [12, 28]. Thus, pancreatic cancer cells appear to be particularly dependent on PI3K and mTOR signaling for their survival, an observation highlighting the tissue-type specificity of therapeutically relevant signal transduction pathways.

Cell lines undergoing apoptosis in response to treatment with PI3K inhibitors displayed clear evidence of autophagy,

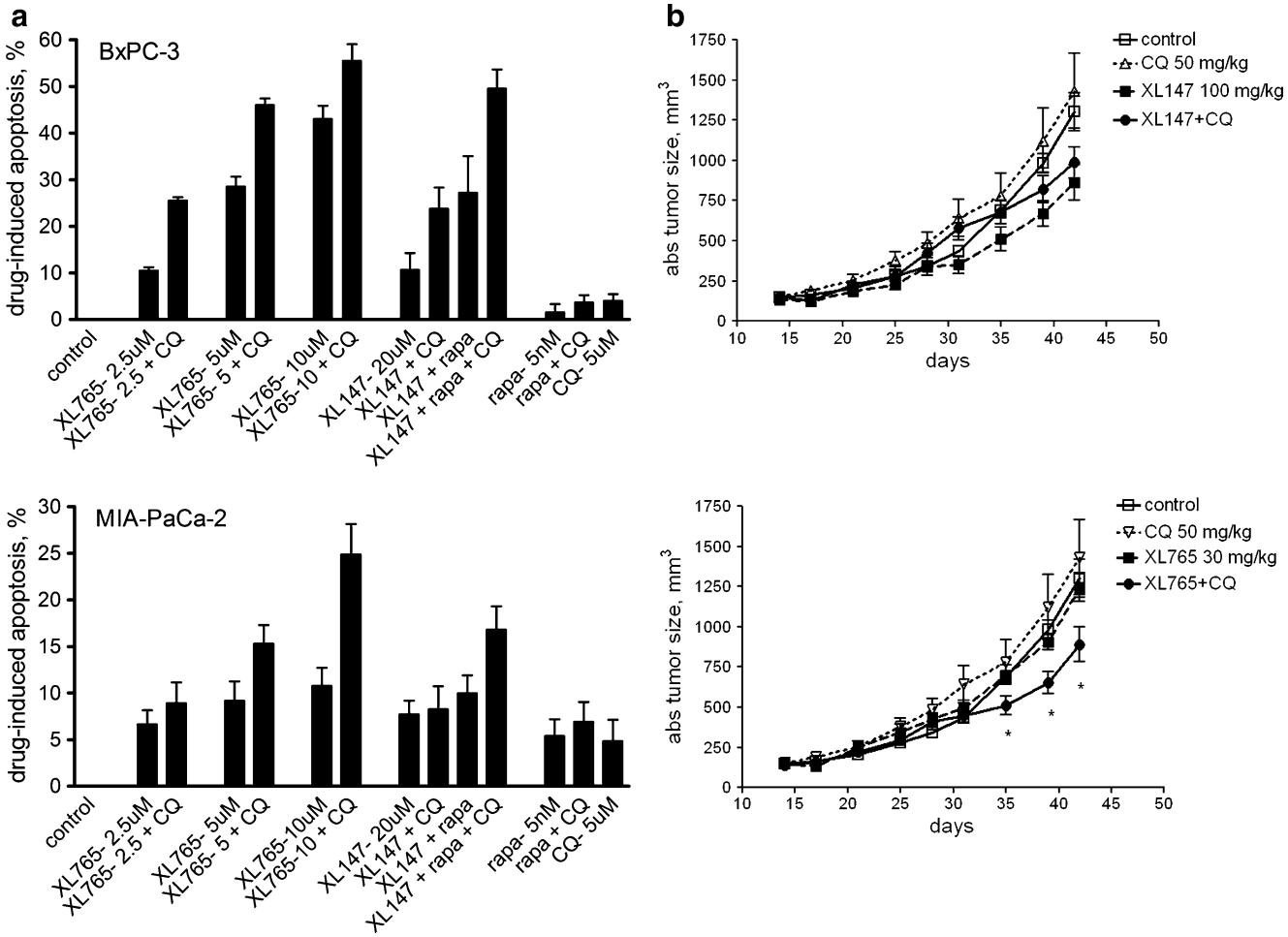

Fig. 6 Apoptosis triggered by PI3K/mTOR inhibitors in enhanced by autophagy inhibitor chloroquine (*CQ*) in vitro **(a)** and in vivo **(b)**. **a** BxPC-3 and MIAPaCa-2 cells were preincubated with CQ for 1 h then treated with different doses of XL765, XL147, or XL147+rapamycin combination. Cells were harvested at 72 h post-drug treatment, stained with annexin V/PI and analyzed by FACS to determine the percentage of total annexin V-positive cells as percentage of apoptotic cells. Apoptosis of untreated control population was subtracted from the drug-treated population to determine the drug-induced apoptosis. *Columns*, mean of duplicates; *bars*, SD. For each duplicate, 40,000 cells were acquired. The results were confirmed in three independent experiments. **b** Combined inhibition of PI3K/mTOR signal transduction and autophagy inhibits tumor growth in vivo. BxPC-3 pancreatic cancer xenografts were established in mice. Animals were given XL765, XL147, chloroquine alone or in combination and tumor growth was monitored for 28 days. Eight animals per group were treated and each data point is a mean of eight tumors, *bars*, SEM. Statistical analysis was performed by using Student's *t* test (two-tailed). Asterisks indicate statistically significant difference, P value<0.05

a catabolic process whereby cells autodigest cellular organelles for energy production [29]. Opposing effects of autophagy on cell survival have been described in cancer cells. For example, induction of autophagy prevented death receptor-mediated apoptosis in sarcoma cells [30]. In contrast, pharmacological inhibition of autophagy resulted in increased apoptosis rates in a variety of models, including glioblastoma treated with temozolomide [22, 31]. In the case of our pancreatic cancer cell line panel, inhibition of autophagy resulted in significantly increased rates of apoptotic cell death, in particular in cells treated with dual-targeted inhibitors. Thus, our data demonstrate a strong cooperative effect of PI3K and mTOR inhibition on induction of autophagy. While phosphorylation of S6 kinase, a substrate of mTORC1, was strongly inhibited in cells treated with rapamycin, 4EBP1 phosphorylation remained unaffected. In contrast, dual inhibition of PI3K and mTOR abolished phosphorylation of this protein, while inhibition of PI3K alone did not impact phosphorylation of S6K. Thus, interruption of mTORC1-dependent and independent signaling is required for activation of autophagy. It is of interest that induction of the pro-survival mechanism autophagy was most pronounced in those cells that also displayed evidence of apoptosis. This observation is consistent with a dual role of the AKT, which is well known to suppress apoptosis by inhibiting FoxO proteins [32] and to suppress autophagy through inhibition of FoxO3 [33], and by increasing mitochondrial superoxide as well as reactive oxygen species [34].

Inhibition of autophagy resulted in enhanced apoptosis in vitro and in vivo following treatment with PI3K inhibitors, in particular dual-targeted PI3K/mTOR inhibitors, which are currently undergoing clinical evaluation. It is important to note that in our in vivo model, administration of XL765 alone did not inhibit tumor growth. This observation is in agreement with published results obtained with NVP-BEZ235, a dual-targeted PI3K/mTOR inhibitor, in a primary xenograft model of human pancreatic cancer [14]. In contrast, XL765 in combination with chloroquine resulted in significant inhibition of tumor growth. These data strongly suggest clinical evaluation of this combination, in particular in pancreatic cancer, a disease for which novel therapeutic approaches are urgently needed.

Acknowledgments We thank UCSF Laboratory for Cell Analysis and Preclinical Therapeutics Cores.

Conflicts of interest D. Aftab is an employee and a shareholder of Exelixis, Inc. and W.M. Korn received research funding from Exelixis, Inc.

References

1. Downward J (2003) Targeting RAS signalling pathways in cancer therapy. Nat Rev Canc 3:11–22
2. Agbunag C, Bar-Sagi D (2004) Oncogenic K-ras drives cell cycle progression and phenotypic conversion of primary pancreatic duct epithelial cells. Canc Res 64:5659–5663
3. Sawyers CL (2009) Finding and drugging the vulnerabilities of RAS-dependent cancers. Cell 137:796–798
4. Asano T, Yao Y, Zhu J, Li D, Abbruzzese JL, Reddy SA (2004) The PI 3-kinase/Akt signaling pathway is activated due to aberrant Pten expression and targets transcription factors NF-kappaB and c-Myc in pancreatic cancer cells. Oncogene 23:8571–8580
5. Altomare DA, Tanno S, De Rienzo A, Klein-Szanto AJ, Skele KL, Hoffman JP, Testa JR (2002) Frequent activation of AKT2 kinase in human pancreatic carcinomas. J Cell Biochem 87:470–476
6. Chadha KS, Khoury T, Yu J, Black JD, Gibbs JF, Kuvshinoff BW, Tan D, Brattain MG, Javle MM (2006) Activated Akt and Erk expression and survival after surgery in pancreatic carcinoma. Ann Surg Oncol 13:933–939
7. Rinehart J, Adjei AA, Lorusso PM, Waterhouse D, Hecht JR, Natale RB, Hamid O, Varterasian M, Asbury P, Kaldjian EP et al (2004) Multicenter phase II study of the oral MEK inhibitor, CI-1040, in patients with advanced non-small-cell lung, breast, colon, and pancreatic cancer. J Clin Oncol 22:4456–4462
8. Patnaik A, LoRusso P, Tabernero JA, Laird D, Aggarwal S, Papadopoulos K (2007) Biomarker development for XL765, a potent and selective oral dual inhibitor of PI3K and mTOR currently being administered to patients in a Phase I clinical trial. Molecular Targets and Cancer Therapeutics Conference, San Francisco, pp. B265
9. Feldman ME, Apsel B, Uotila A, Loewith R, Knight ZA, Ruggero D, Shokat KM (2009) Active-site inhibitors of mTOR target rapamycin-resistant outputs of mTORC1 and mTORC2. PLoS Biology 7:e38
10. Garcia-Martinez JM, Moran J, Clarke RG, Gray A, Cosulich SC, Chresta CM, Alessi DR (2009) Ku-0063794 is a specific inhibitor of the mammalian target of rapamycin (mTOR). Biochem J 421:29–42
11. Yu K, Toral-Barza L, Shi C, Zhang WG, Lucas J, Shor B, Kim J, Verheijen J, Curran K, Malwitz DJ et al (2009) Biochemical, cellular, and in vivo activity of novel ATP-competitive and selective inhibitors of the mammalian target of rapamycin. Canc Res 69:6232–6240
12. Fan QW, Knight ZA, Goldenberg DD, Yu W, Mostov KE, Stokoe D, Shokat KM, Weiss WA (2006) A dual PI3 kinase/mTOR inhibitor reveals emergent efficacy in glioma. Canc Cell 9:341–349
13. Brachmann SM, Hofmann I, Schnell C, Fritsch C, Wee S, Lane H, Wang S, Garcia-Echeverria C, Maira SM (2009) Specific apoptosis induction by the dual PI3K/mTor inhibitor NVP-BEZ235 in HER2 amplified and PIK3CA mutant breast cancer cells. Proceedings of the National Academy of Sciences of the United States of America 106: 22299–22304
14. Cao P, Maira SM, Garcia-Echeverria C, Hedley DW (2009) Activity of a novel, dual PI3-kinase/mTor inhibitor NVP-BEZ235 against primary human pancreatic cancers grown as orthotopic xenografts. Br J Canc 100:1267–1276
15. Knight ZA, Gonzalez B, Feldman ME, Zunder ER, Goldenberg DD, Williams O, Loewith R, Stokoe D, Balla A, Toth B et al (2006) A pharmacological map of the PI3-K family defines a role for p110alpha in insulin signaling. Cell 125:733–747
16. Gysin S, Rickert P, Kastury K, McMahon M (2005) Analysis of genomic DNA alterations and mRNA expression patterns in a panel of human pancreatic cancer cell lines. Gene Chromosome Canc 44:37–51
17. Mirzoeva OK, Das D, Heiser LM, Bhattacharya S, Siwak D, Gendelman R, Bayani N, Wang NJ, Neve RM, Guan Y et al (2009) Basal subtype and MAPK/ERK kinase (MEK)-phosphoinositide 3-kinase feedback signaling determine susceptibility of breast cancer cells to MEK inhibition. Canc Res 69:565–572
18. Fung C, Lock R, Gao S, Salas E, Debnath J (2008) Induction of autophagy during extracellular matrix detachment promotes cell survival. Mol Biol Cell 19:797–806
19. Shigemitsu K, Tsujishita Y, Hara K, Nanahoshi M, Avruch J, Yonezawa K (1999) Regulation of translational effectors by amino acid and mammalian target of rapamycin signaling pathways. Possible involvement of autophagy in cultured hepatoma cells. J Biol Chem 274:1058–1065
20. Kalamidas SA, Kondomerkos DJ, Kotoulas OB, Hann AC (2004) Electron microscopic and biochemical study of the effects of rapamycin on glycogen autophagy in the newborn rat liver. Microsc Res Tech 63:215–219
21. Kabeya Y, Mizushima N, Ueno T, Yamamoto A, Kirisako T, Noda T, Kominami E, Ohsumi Y, Yoshimori T (2000) LC3, a mammalian homologue of yeast Apg8p, is localized in autophagosome membranes after processing. EMBO J 19:5720–5728
22. Kanzawa T, Germano IM, Komata T, Ito H, Kondo Y, Kondo S (2004) Role of autophagy in temozolomide-induced cytotoxicity for malignant glioma cells. Cell Death Differ 11:448–457
23. Kim J, Klionsky DJ (2000) Autophagy, cytoplasm-to-vacuole targeting pathway, and pexophagy in yeast and mammalian cells. Annu Rev Biochem 69:303–342
24. Eisenberg-Lerner A, Bialik S, Simon HU, Kimchi A (2009) Life and death partners: apoptosis, autophagy and the cross-talk between them. Cell Death Differ 16:966–975
25. Ma L, Chen Z, Erdjument-Bromage H, Tempst P, Pandolfi PP (2005) Phosphorylation and functional inactivation of TSC2 by Erk implications for tuberous sclerosis and cancer pathogenesis. Cell 121:179–193
26. Carriere A, Cargnello M, Julien LA, Gao H, Bonneil E, Thibault P, Roux PP (2008) Oncogenic MAPK signaling stimulates mTORC1 activity by promoting RSK-mediated raptor phosphorylation. Curr Biol 18:1269–1277
27. Raynaud FI, Eccles S, Clarke PA, Hayes A, Nutley B, Alix S, Henley A, Di-Stefano F, Ahmad Z, Guillard S et al (2007) Pharmacologic characterization of a potent inhibitor of class I phosphatidylinositide 3-kinases. Canc Res 67:5840–5850

28. Faber AC, Li D, Song Y, Liang MC, Yeap BY, Bronson RT, Lifshits E, Chen Z, Maira SM, Garcia-Echeverria C, Wong KK, Engelman JA (2009) Differential induction of apoptosis in HER2 and EGFR addicted cancers following PI3K inhibition. Proceedings of the National Academy of Sciences of the United States of America 106: 19503–19508
29. Levine B (2005) Eating oneself and uninvited guests: autophagy-related pathways in cellular defense. Cell 120:159–162
30. Djavaheri-Mergny M, Amelotti M, Mathieu J, Besancon F, Bauvy C, Souquere S, Pierron G, Codogno P (2006) NF-kappaB activation represses tumor necrosis factor-alpha-induced autophagy. J Biol Chem 281:30373–30382
31. Boya P, Gonzalez-Polo RA, Casares N, Perfettini JL, Dessen P, Larochette N, Metivier D, Meley D, Souquere S et al (2005) Inhibition of macroautophagy triggers apoptosis. Mol Cell Biol 25:1025–1040
32. Greer EL, Brunet A (2005) FOXO transcription factors at the interface between longevity and tumor suppression. Oncogene 24:7410–7425
33. Zhao J, Brault JJ, Schild A, Goldberg AL (2008) Coordinate activation of autophagy and the proteasome pathway by FoxO transcription factor. Autophagy 4:378–380
34. Degtyarev M, De Maziere A, Orr C, Lin J, Lee BB, Tien JY, Prior WW, van Dijk S, Wu H, Gray DC et al (2008) Akt inhibition promotes autophagy and sensitizes PTEN-null tumors to lysosomotropic agents. J Cell Biol 183:101–116

Grant Support

UC Discovery Grant bio07-10664 (W.M. Korn), Exelixis, Inc. (W.M. Korn).